Available online at www.sciencedirect.com

ScienceDirect

Materials Chemistry and Physics 102 (2007) 281–283

MATERIALS CHEMISTRY AND PHYSICS

www.elsevier.com/locate/matchemphys

Growth and holographic storage properties of In:Ce:Cu:LiNbO_3 crystal

Yiran Nie[a,*], Rui Wang[b], Biao Wang[a,c]

[a] Department of Aerospace Engineering and Mechanics and Electro-Optics Technology Center,
Harbin Institute of Technology, Harbin 150001, PR China
[b] Department of Applied Chemistry and Electro-Optics Technology Center,
Harbin Institute of Technology, Harbin 150001, PR China
[c] State Key Laboratory of Optoelectronic Materials and Technologies, School of Physics and Engineering,
Sun Yat-sen University, Guangzhou 510275, PR China

Received 20 November 2005; received in revised form 23 September 2006; accepted 16 January 2007

Abstract

A series of In:Ce:Cu:LiNbO_3 crystals with different concentration of In_2O_3 were grown by the Czochralski method. The infrared transmission spectra and the photo-damage resistant ability of the crystals were measured. The OH^- absorption peak of In(3 mol%):Ce:Cu:LiNbO_3 crystal shifts to ultraviolet. The photo-damage resistant ability of In(3 mol%):Ce:Cu:LiNbO_3 crystal is about two orders of magnitude higher than those of pure LiNbO_3 and Ce:Cu:LiNbO_3 crystals. The diffraction efficiency, response time of In:Ce:Cu:LiNbO_3 crystals were tested by two-wave coupling experiment. The response time of In(3 mol%):Ce:Cu:LiNbO_3 crystal only one fourth of that of Ce:Cu:LiNbO_3. The mechanism of OH^- absorption peak shifting and photo-damage resistant ability enhancement were discussed.

Keywords: In:Ce:Cu:LiNbO_3; Holographic storage; Infrared transmission spectra

1. Introduction

Lithium niobate (LiNbO_3) single crystal has been widely used for its unique electro-optic, acousto-optic and nonlinear optical properties [1,2]. The most important application is holographic storage because of its excellent photo-refractive properties [3,4]. Holographic storage devices using LiNbO_3 crystals as the storage substrate can achieve large capability holographic storage. Nowadays, people adopt non-volatile holographic storage to maintain the information for a long time in this photo-refractive crystal. The two-photon fixed method is a new technique to achieve the non-volatile holographic storage. Two dopants with different energy levels are doped into LiNbO_3 crystal. The electrons can be excited from the deeper level to the shallower level by the high laser energy and all electrons in the shallow level (including excited ones from deep level) are used for storage. Using Mn:Fe:LiNbO_3 and Ce:Cu:LiNbO_3 crystals [5,6], the non-volatile holographic storage has been achieved by means of the two-photon fixed method.

However, it is found that Ce:Cu:LiNbO_3 has two shortcomings: low photo-damage resistant ability and long response time, which severely limit its applications [7,8]. The holographic storage properties of the LiNbO_3 crystal can be greatly improved by doping with MgO [9,10], ZnO [11,12], or In_2O_3 [13,14], Sc_2O_3 [15,16]. In this paper, we propose to dope In_2O_3, CeO_2 and CuO into LiNbO_3 to grow In:Ce:Cu:LiNbO_3 crystals. Ce and Cu are doped to act as the deeper and shallower energy levels in the non-volatile holographic storage. In^{3+} is doped to improve the photo-damage resistant ability and shorten the response time.

2. Experimental

2.1. Preparation of crystal samples

In(3 mol%):Ce:Cu:LiNbO_3, In(2 mol%):Ce:Cu:LiNbO_3, In(1 mol%):Ce:Cu:LiNbO_3 crystals were grown by the Czochralski method. The intermediate frequency furnace was used as the heater. The starting materials were Li_2CO_3, Nb_2O_5, In_2O_3, CeO_2 and CuO with the purity of 99.99%. The Li/Nb ratio of the initial melts to grow the congruent LiNbO_3 is 0.946. The concentrations of Ce and Cu are 0.1 and 0.03 wt.%, respectively. The concentrations of In^{3+} are 1, 2 and 3 mol%, respectively. To prepare the polycrystalline, these materials were mixed thoroughly, calcinated at 850 °C for 4 h, and sintered at 1150 °C for 4 h. The technology conditions for crystal growth were as follow: pulling rate of 2 mm h^{-1}, rotation rate of 20 rpm and temperature gradient of

---

[*] Corresponding author. Tel.: +86 20 84113370; fax: +86 20 84115692.
E-mail address: nieyiran@hit.edu.cn (Y. Nie).

0254-0584/$ – see front matter © 2007 Elsevier B.V. All rights reserved.
doi:10.1016/j.matchemphys.2007.01.009

Table 1
The compositions of the samples

Crystal	1#	2#	3#	4#	$LiNbO_3$
In^{3+} in melt (mol%)	1.0	2.0	3.0	0	0
In^{3+} in crystal (mol%)	0.703	1.296	1.852	0	0
k of In^{3+}	0.703	0. 648	0.617	–	–
Ce^{4+} in melt (wt.%)	0.1	0.1	0.1	0.1	0
Cu^{2+} in melt (wt.%)	0.03	0.03	0.03	0.03	0

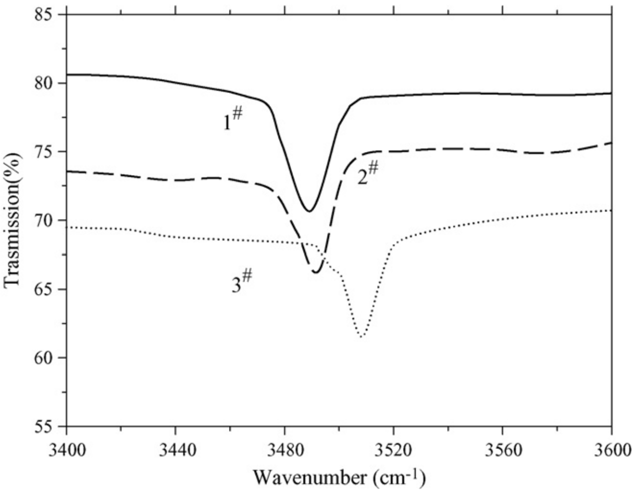

Fig. 1. Infrared transmission spectra of the samples.

30–40 °C cm^{-1}. The diameters and heights of these crystals were about 30 and 50 mm, respectively. The as-grown crystals were poled in another furnace where the temperature was held at about 1200 °C for 4 h with an applied direct current of 5 mA cm^{-2}. Then the crystals were cut into samples of 15 mm × 10 mm × 2 mm. Then all the wafers were polished to optical grade. The compositions of the samples were listed in Table 1.

2.2. *Properties measurements*

The concentrations of In^{3+} in the $In:Ce:Cu:LiNbO_3$ crystals were measured by inductively coupled plasma atomic-emission spectrometry (ICP-AES). The distribution coefficient (k) of In^{3+} was calculated by comparing the In^{3+} concentration in the crystal and the initial In^{3+} concentration in the melt. The results are listed in Table 1.

The infrared transmission spectra at room temperature ranging from 3000 to 4000 cm^{-1} were obtained with a Fourier IR spectrometer. Infrared transmission spectra at the partial range from 3400 to 3600 cm^{-1} are shown in Fig. 1.

The facula-distortion observing method was applied to measure the photo-damage resistant ability of the crystals. The experimental set-up is shown in Fig. 2. The Ar^+ laser (λ = 488.0 nm) was employed as the light source, and the output intensity of the beam could be regulated. The beam transited the light shed and convex lens and then focused on the sample. The focula could be observed on the screen. The polarization direction of the beam was along the c-axis of the crystal. When the power intensity was low, there was no photo-damage and the facula was round. When the power intensity achieved a certain value (the threshold value), the facula began to elongate along the c-axis of the crystal. The photo-damage occurred and the power density of the output beam was recorded by the power detector. This value is defined as the photo-damage threshold (R), which is a parameter to evaluate the photo-damage resistance ability of the crystal. The higher the photo-damage resistant ability is, the larger signal-noise ratio the crystal has. The results are shown in Table 2.

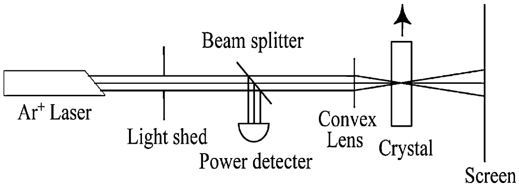

Fig. 2. Set-up for measurement of photo-damage resistant ability.

Table 2
Photo-damage resistant abilities (R) of the samples

Sample	R ($W cm^{-2}$)
1#	9.3×10^2
2#	1.4×10^3
3#	2.6×10^4
4#	1.7×10^2
$LiNbO_3$	1.9×10^2

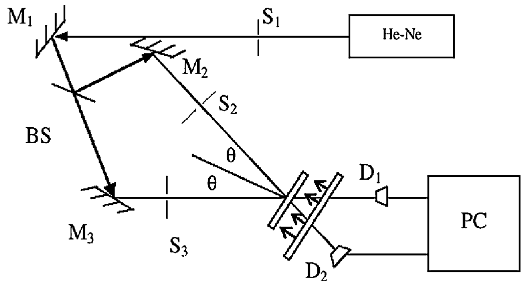

Fig. 3. Sketch of two-wave coupling optical path. M_1, M_2, M_3: mirrors; BS: beam splitter; D_1, D_2: detector; S_1, S_2, S_3: diaphragm; PC: computer.

Table 3
The holographic storage properties of $In:Ce:Cu:LiNbO_3$

Samples	η_{max} (%)	τ_w (s)	τ_e (s)	τ (s)
4#	62	220	610	134
1#	56	160	580	97
2#	53	118	426	74
3#	48	60	295	38

The diffraction efficiency and the response time of the $In:Ce:Cu:LiNbO_3$ crystals were measured by the two-wave coupling experiments. The optical path was shown in Fig. 3. The He–Ne laser (λ = 632.8 nm) was used as the light source in the experiment. The polarizing of the output beam was in the incident plane. The beam was separated two by the beam splitter. One is signal light I_s and the other is reference light I_r. The intensity of $I_r = I_s = 150\ mW\ cm^{-2}$ and their crossing angle is 10°–30°. The diffraction efficiency η is defined as the ratio of the diffraction light intensity I_{sd} to the transmitted light intensity I_{st} for the signal light. The response time τ is defined as the time from the light begins radiating to the diffraction efficiency η is up to $(1 - \exp(-1))$ of its maximum (η_{max}). The writing time τ_w and the erasing time τ_e can be also gotten. The experiment results are shown in Table 3.

3. Results and discussion

The Infrared transmission spectra of the samples are shown in Fig. 1. For $LiNbO_3$ crystal with ABO_3 form structure, H^+ ions can come into the lattices and combines with O^{2-} ions to form OH^-. The shifting of OH^- absorption peak reflects the location and threshold concentration of the doped ions. From Fig. 1, it can be seen that the OH^- absorption peaks of $1^\#$ and $2^\#$ samples are located at about 3486 cm^{-1}, while that of $3^\#$ sample shifts to 3507 cm^{-1}. The OH^- absorption peaks of the crystals with low In^{3+} concentration are similar as that of pure congruent $LiNbO_3$ crystal, which is located about 3484 cm^{-1} [17,18].

From the viewpoint of Li-vacancy model, there are Li^+ vacancies and antisite Nb $(Nb_{Li})^{4+}$ defects in congruent pure $LiNbO_3$ crystal and the OH^- absorption spectra reflect the change of the defects structure[19–21]. The OH^- vibration absorption peak of pure congruent $LiNbO_3$ crystal located at 3484 cm^{-1} mainly reflects the vibration condition of OH^- around Li^+ vacancies. In the case of In:Ce:Cu:$LiNbO_3$ crystals, when In^{3+} concentration is below its threshold concentration, In^{3+} ions occupy antisite Nb $(Nb_{Li})^{4+}$ or Li^+ vacancies, and exist in the form of $(In_{Li})^{2+}$. They are repellent to H^+ ions. In this case, the OH^- still vibrate around Li^+ vacancies, so the absorption peaks of $1^\#$ and $2^\#$ samples are similar as that of pure $LiNbO_3$ crystal. When In^{3+} concentration is above its threshold concentration, the additional In^{3+} ions begin to occupy Nb-site and exist in the form of $(In_{Nb})^{2-}$. Because $(In_{Nb})^{2-}$ have stronger attraction to H^+ than that of Li^+ vacancies. So H^+ ions collect around $(In_{Nb})^{2-}$ and the absorption peak of $3^\#$ sample mainly reflects the vibration condition of OH^- around $(In_{Nb})^{2-}$.

The results of the photo-damage resistant ability of In:Ce:Cu:$LiNbO_3$ crystals are shown in Table 2. It can be seen that the photo-damage resistant ability of In(3 mol%):Ce:Cu:$LiNbO_3$ crystal is about two orders of magnitude higher than those of pure $LiNbO_3$ and Ce:Cu:$LiNbO_3$ crystals. From the analysis above, we know that the In^{3+} ions begin to occupy Nb-site when In^{3+} concentration is above its threshold concentration. At the same time, the Ce^{4+} and Cu^{2+} ions occupy Nb-site, too. They exit in the form of $(In_{Nb})^{2-}$, $(Ce_{Nb})^-$ and $(Cu_{Nb})^{3-}$. Their abilities to capture electrons decrease and the photoconductivity of In(3 mol%):Ce:Cu:$LiNbO_3$ crystal increases rapidly. According to the Scalar expression, $\delta\Delta n \approx B\kappa\alpha I/\sigma$ [22], where B is the generalized electro-optical coefficient, κ is the glass constant, α is the optical absorption coefficient, I is the intensity of the light and σ is the conductivity ($\sigma = \sigma_d + \sigma_p$, σ_d is the dark conductivity and σ_p is the photoconductivity, $\sigma_d \ll \sigma_p$, so $\sigma \approx \sigma_p$), the photorefractive ability of the $LiNbO_3$ crystal increases with the decrease of the photoconductivity. So with the increasing of the photoconductivity, the photo-damage resistant ability of In(3 mol%):Ce:Cu:$LiNbO_3$ improves obviously.

The results of holographic storage properties of In:Ce:Cu:$LiNbO_3$ are shown in Table 3. As holographic storage materials, the crystals should possess high diffraction efficiency to represent the recorded images clearly. The shorter response time can improve the efficiency. From the results shown in Table 3, the response time of In(3 mol%):Ce:Cu: $LiNbO_3$ is about one fourth of that of Ce:Cu:$LiNbO_3$ crystal, though the diffraction efficiency has a little decrease. The In(3 mol%):Ce:Cu:$LiNbO_3$ crystal is more suitable for holographic storage.

4. Conclusions

The Ce:Cu:$LiNbO_3$ crystal has two drawbacks: low photo-damage resistant ability and long response time. By doping In_2O_3 in Ce:Cu:$LiNbO_3$ crystal to grow In:Ce:Cu:$LiNbO_3$ crystal, the photo-damage resistant ability increase two orders of magnitude higher and the response speed increases four times higher than those of Ce:Cu:$LiNbO_3$ crystal, when the In^{3+} concentration reach its threshold concentration. In(3 mol%):Ce:Cu:$LiNbO_3$ crystal is a more potential holographic storage material compared with Ce:Cu:$LiNbO_3$ crystal.

Acknowledgements

This work was supported by the National Natural Science Foundation of China (50232030, 10572155, 10172030) and the Science Foundation of Guangzhou Province (2005A10602002).

References

[1] P. Guner, J.P. Huignard, Photorefractive Materials Their Application, Topics of Applied Physics, vol. 62, Springer, Berlin, 1998.
[2] A.M. Prokhorov, Y.S. Kuzminov, Physics and Chemistry of crystalline Lithium Niobate, Hilger, Bristol, 1990.
[3] K. Buse, A. Adibi, D. Psaltis, J. Opt. Soc. Am. B 18 (2001) 584.
[4] S. Chen, J.T. Lamacchia, D.B. Frazer, Appl. Phys. Lett. 13 (2) (1968) 223.
[5] K. Buse, A. Adibi, D. Psaltis, Nature 393 (1998) 665.
[6] B. Wang, R. Wang, Y. Nie, Opt. Mater. 23 (2003) 273.
[7] Y. Furukawa, K. Kitamura, S. Takekawa, A. Miyamoto, M. Terao, N. suda, Appl. Phys. Lett. 77 (2000) 2494.
[8] Y. Liu, L. Liu, C. Zhou, L. Xu, Opt. Lett. 25 (2000) 908.
[9] D.A. Bryan, R. Gerson, H.E. Tomaschke, Appl. Phys. Lett. 44 (1984) 847.
[10] L. Palfalvi, G. Almasi, J. Hebling, A. Peter, K. Polar, Appl. Phys. Lett. 80 (13) (2002) 2245.
[11] T.R. Volk, V.I. Pryalkin, N.M. Rubinina, Opt. Lett. 15 (1990) 996.
[12] T.R. Volk, M.A. Ivanov, V.I. Prylkin, N.M. Rubinina, Ferroelectrics 126 (1992) 57.
[13] Y. Kong, J. Wen, H. Wang, Appl. Phys. Lett. 66 (1995) 280.
[14] T.R. Volk, N.M. Rubinina, Ferroelectr. Lett. 14 (1992) 37.
[15] J.K. Yamamoto, K. Kitamuta, N. Lyi, S. Kimura, Y. Furukawa, M. Sato, Appl. Phys. Lett. 61 (18) (1992) 2156.
[16] M. Nakamura, S. Takekawa, Y.W. Liu, K. Kitamuta, Jpn J. Appl. Phys. 43 (2004) 947.
[17] L. Kovacs, M. Wohlecke, A. Jovanovic, K. Polgar, S. Kapphan, J. Phys. Chem. 52 (1991) 797.
[18] T. Volk, M. Wohlecke, N. Rubinina, N.V. Razumovski, F. Jermann, C. Fischer, J. Lumin, Appl. Phys. A 60 (1995) 217.
[19] N. Lyi, K. Kitamura, F. Izumi, J.K. Yamamoto, T. Hayashi, H. Asano, S. Kimura, J. Solids State Chem. 101 (1992) 340.
[20] Y. Kong, W. Zhang, J. Xu, et al., Infrared Phys. Technol. 45 (2004) 281–289.
[21] P. Sen, P.K. Sen, R. Bhatt, et al., Solid State Commun. 129 (2004) 747–752.
[22] T. Volk, N. Rubinina, M. Wöhlecke, J. Opt. Soc. Am. B 11 (1994) 1681.